von KARMAN INSTITUTE
FOR FLUID DYNAMICS

TECHNICAL NOTE 54

TURBULENT FLOW SEPARATION AHEAD OF FORWARD FACING STEPS IN SUPERSONIC TWO-DIMENSIONAL AND AXISYMMETRIC FLOWS

by

H. T. UEBELHACK

RHODE-SAINT-GENESE, BELGIUM

JULY 1969

von Karman Institute for Fluid Dynamics

(14) VKI-TN-54

(9) Technical Note, 54

(6) TURBULENT FLOW SEPARATION AHEAD OF FORWARD FACING STEPS IN SUPERSONIC TWO-DIMENSIONAL AND AXISYMMETRIC FLOWS.

by

(10) H. T. UEBELHACK

(11) July 69 12. 44p.

SUMMARY

Pressure distributions in the separated flow region ahead of forward facing steps and on the step face in supersonic turbulent flows obtained at VKI are compared with those found by previous investigators. The following geometries were investigated :

1. Flat plate step models which
   (a) spanned the tunnel completely
   (b) spanned 75% of the tunnel width.
2. Cone-Cylinder-step models.
3. Axisymmetric internal flow models
   (a) nozzles followed by a 90° contraction
   (b) ejectors with a 90° contraction of the supersonic diffuser.

Parameters such as step height, unit Reynolds number and Mach number were compared. It was intended, in particular, to relate the axisymmetric results to existing two-dimensional data.

A general law relating the variation of the step pressure integral with Mach number was found by analyzing pressure distributions on the step face.

The influence of flow inclination, Mach number variation and three-dimensional effects on the characteristic pressures were discussed. The flow has been visualized by schlieren and schadow photographs and by the oil flow technique.

TABLE OF CONTENTS

LIST OF SYMBOLS

A	cross-section
C_p	pressure coefficient
d,D	diameter
D	$=\int p dy$ pressure integral
Fi	induced side force
h	step height
L	model length
M	Mach number
p	pressure
Re	Reynolds number
x	coordinate in flow direction
y	step coordinate
α	angle of incidence
θ	flow angle
δ	boundary layer thickness

Subscripts

$0\ \infty$	free stream stagnation conditions
1	before interaction
ne	nozzle exit
p	first peak
s	separation
*	throat section
**	second throat

1. INTRODUCTION

The phenomenon of flow separation ahead of forward facing steps and similar obstacles has been studied experimentally during the past fifteen years mostly in the context of other types of separation induced by pressure gradients caused by shock waves, or ramps. (Refs.1,2). In aerodynamic designs , steps and sudden enlargements of the cross-section are usually avoided because of the high drag of these geometries. There are, however, a few cases where a sudden change of the flow direction and separation cannot be avoided such as the interaction between the outer flow and the boundary of an underexpanded jet at the exit of a rocket nozzle, gas or fuel injection into a supersonic stream (Refs.3,4) or three-dimensional obstacles at the surface of an aerodynamic body (Refs.5,6). In all those cases, the study of flow separation ahead of the obstacles becomes indispensable in order to predict the drag and the side forces caused by the pressure distribution in the separated flow region.

Other technical applications of a rather sudden change in cross-section are supersonic diffusers (second throats) in supersonic wind tunnels and in supersonic diffusers of ejectors. Here a high contraction angle is often desired because a long ramp would interfere with the shock wave pattern of the central flow. The pressure distribution on the contraction has to be known in order to predict the efficiency and the pressure recovery of a second throat.

Experiments on second throat diffusers of ejectors have shown that a sudden contraction of the cross-section (forward facing step) displays the same improvement in pressure recovery as a ramp type contraction (Ref.7). Parameters like the ramp angle of the second throat, the axial

location of the ramp and the possible occurence of separation ahead of the ramp complicate the analysis of the problem. In the case of a sudden contraction (step) the flow forms its "natural ramp" by the process of separation.

The interest of the author in this field has lead to a study of flow separation ahead of forward facing steps in order to :

i compare axisymmetric internal and external flow data, particularly in the case of flows over cavities, with two-dimensional results;

ii explain the scatter of available experimental data and discuss the experimental difficulties;

iii predict the pressure distribution and the pressure integral over the step face;

iv visualize and examine the separated flow region;

v find a suitable reattachment criteria for this particular problem.

2. REVIEW OF RESULTS OF PREVIOUS INVESTIGATORS

Turbulent flow separation ahead of forward facing steps and comparable obstacles were studied in the past mainly on flat plate step models which spanned the wind tunnel or which had side fences and on similar models with free ends (about 75% of the available data) (Refs.1,2,8,9,10,11,12). Other data were obtained on models such as two- and three-dimensional flow injection into uniform flow (Refs.3,4) and three-dimensional obstacle on flat plate models (Ref.5). A summary of the most important available data is given in Ref. 13. The main features of this type of flow and the essential phenomena should be briefly summarized here :

The wall pressure distribution in the separated flow region, including the step face, at sufficiently high Reynolds numbers always shows a similar variation. A Reynolds number range from $Re_\delta = 3.10^4 \ldots 2.10^6$ have been investigated so far :

The wall pressure rises in a steep gradient from the point where the interaction is felt first up to a first peak value which is situated at about 50% of the separated length. The wall pressure then decays towards the step and rises again reaching about 1.4 times the value of the first peak pressure in the corner. On the step face towards the outer corner, it decays again to a minimum of about 1.2 times the first peak value between 30 and 40% of the step height and then rises continuously reaching 2...3 times p_D at the outer edge of the step. In the outer 20% of the step height the pressure distributions seems to be strongly influenced by the Mach number and the relative step height, Refs.4,5.

Primary attention in the previous experiments has been paid to the value of the first peak pressure in the separated flow region and its dependence on Mach number and

Reynolds number. All the experimentations have found rising peak pressure ratios p_p/p_1 with rising initial Mach numbers M_1. A Mach number range between 1.4 and 6 has been investigated experimentally so far. The peak pressure ratio p_p/p_1 scatters around a mean value by about $\pm$ 10%. In Ref.8, the mean value has been approximated by

$$C_{p_p} = \frac{p_p - p_1}{\frac{1}{2}\gamma p_1 M_1^2} = \frac{3.2}{\gamma+(M_1+1)} \qquad (1)$$

which represents the average value rather well particularly at low supersonic Mach numbers and up to $M_1=3.5$. Beyond $M_1=5$ there are only few data available (Ref.10). In order to represent the mean value also at high Mach numbers

$$\frac{p_p - p_1}{p_1} = \frac{1}{2} M_1 \qquad (2)$$

is suggested in Ref.13.

An aerodynamically based method to predict the first peak pressure would be the pressure rise across an oblique two-dimensional shock wave, analogous to the separation phenomenon at rearward facing steps where the base pressure is determined by the deviation of the outer flow in the expansion fan at the corner. The peak pressure ratio then is given by

$$\frac{p_p}{p_1} = \frac{2\gamma}{\gamma+1} (M_1^2 \sin^2\theta_s - 1) \qquad (3)$$

It has been observed that the separation angle, i.e. the angle between the wall and the straight dividing streamlines from separation to reattachment very close to the outer corner of the step, is roughly constant and scatters around 13°. Eq.(3) averages well the peak pressure ratio between

M_1 = 2 and 5. As mentioned before there are not enough data available beyond M_1 = 5 in order to speak of a mean value.

The Reynolds number dependence of the peak pressure has been examined particularly in Refs.2,8,9. It was found that there was almost no dependence on Reynolds number in turbulent flow when the initial Reynolds number is sufficiently high. The data presented in Ref.2 show a small decrease of p_p with increasing Re. This however could be due to the still transitional behavior of the tripped boundary layer.

The separation pressure p_s has been determined by different techniques such as pitot probes shadowgraphs and oil flow pictures. (Refs.1,2,10). Only a few attempts were made in locating the separation point. As an average of those few measurements the separation pressure is suggested to be approximated (Ref.13) by

$$\frac{p_s - p_1}{p_1} = .73 \frac{p_p - p_1}{p_1} \qquad (4)$$

The pressure integral over the separated flow region ahead of the step has also been a subject of discussion in Ref. 13. There, many separated pressure profiles were examined and a similarity was found in their normalized shape which permits an integration in a general form. For the normalized separation induced side force the following linear dependence on Mach number was found

$$\frac{Fi}{p_1 h} = 2.1\, M_1 \qquad (5)$$

Pressure distributions on the step face itself are only presented in Refs.1 and 4 with a sufficient number of points in order to speak of a pressure distribution.

3. EXPERIMENTAL PROGRAMME AND TEST CONDITIONS

The experimental programm presented here was carried out in two different facilities : a supersonic blowdown tunnel (M=3.5) and an ejector test bench. In the blowdown tunnel axisymmetric cone-cylinder step models and flat plate step models were examined.
In the ejector facility, tests were carried out on steps behind an axisymmetric nozzle, designed for parallel flow and on an arrangement of nozzle and a diffuser with a sudden contraction (cavity).

The experimental programmed consisted in a wall pressure survey in the separated flow region ahead of the steps at stagnation pressures between 8 kg/cm^2 and 17 kg/cm^2 in tunnel S4 and between 18 kg/cm^2 and 30 kg/cm^2 in the ejector test facility.

All the tests in tunnel S4 were carried out at step heights of 5 and 7.5 mm in order to check repeatability and the influence of the step height. The boundary layer thickness was determined from schlieren photographs and was found to be 1.5 to 2 mm. The dependence of characteristic pressures on the angle of incidence of the model has been the subject of a series of experiments on both the two-dimensional and the axisymmetric models.

In the ejector facility the axial distance between nozzle exit and step was varied in order to check the uniformity of the flow and the dependence of the pressure data on the boundary layer development length.

3.1. Facilities

The supersonic blowdown tunnel S4 at VKI was used in the first series of experiments. The wind tunnel was designed for a Mach number of 3.5 in the test section of 100 mm height and 80 mm span. Calibration tests displayed a total Mach number variation of 1 % in vertical direction and 0.5 % in lateral direction at a stagnation pressure of 8 kg/cm^2. An ejector behind the tunnel allows a stagnation pressure range between 1 kg/cm^2 and 18 kg/cm^2. The tunnel is equipped with a schlieren and a shadowgraph system.

The ejector test bench consisted of a settling chamber of 40 mm diameter which was followed by a nozzle designed for uniform flow (15 mm throat diameter, 45, 60, 75 mm exit diameter). The step in this facility was realized by a sudden contraction, 90°, of the diffuser section (75 mm diameter) to a diameter of 62 mm. Thus the step height was 6.5 mm in all configurations. The boundary layer thickness was estimated to be roughly 4 mm by comparing the flow condition to other similar arrangements, where the boundary layer thickness was measured. The stagnation pressure in this facility could be varied between 18 and 30 kg/cm^2.

3.2. Models

The two-dim models used in tunnel S4 were flat plate step mo .h spanned the tunnel completely and which were cut 75 % of the tunnel span in the second series of tests (Fig.1). The geometry of the axisymmetric cone cylinder step models is also given in the same figure. All the models were mounted on a sting and connected to a mechanical system which was used to vary the angle of incidence. The diameter of the pressure taps was

0.8 mm on all the models. The spacing of the pressure taps was 2 mm in average on the two-dimensional and the axisymmetric models. Step heights were, in both cases, 5 and 7.5 mm. The thickness of the turbulent boundary layer was in both cases about 1.5 to 2 mm according to the variation in stagnation pressure. All pressures were measured through a scanning valve system by a 15 psi transducer. The output signal was recorded on "graphispot" recorders.

In the ejector test bench the spacing of the pressure taps (0.8 mm) was 2 mm. The pressure holes were located along a meridian. On the step face (6.5 mm) there were 7 pressure holes. The pressures were sensed over the same system of scanning valves and recorders described above.

4. EXPERIMENTAL RESULTS

4.1. Planar Models

The complete wall pressure distribution on the centerline of the two planar models is shown in Figs.2a,2b,3a,3b for two step heights h = 5 and 7.5 mm and tunnel stagnation pressures between 8 and 17 kg/cm^2. In all figures the scale of the step face coordinate is enlarged four times in order to show more details. The variation of the peak pressure ratio with stagnation pressure (unit Reynolds number) is shown in Fig.4 together with the results of other models. The curves show clearly a small decay of the peak pressure ratio with increasing tunnel stagnation pressure. The variation of Reynolds number at separation is roughly from $4.8.10^7$ to $1.1.10^8$. The peak pressure ratio seems to approach assymptotically a constant value at still higher Reynolds number. The change in the peak pressure ratio measured on planar models is about 10 % (models which spanned the tunnel) and 3 % (models with free ends). Love (Ref.8) has already observed a constant peak pressure in a Reynolds number range between 10^6 and 10^7 at Mach numbers between 1.5 and 2.5.

The peak pressures obtained at the highest Reynolds number employed are shown in Fig.5 together with the results from other models and experimental values by other investigators which came to the author's attention.

The step height had no influence on the peak pressure ratio when the model spanned the tunnel. The peak pressure ratios p_p/p_1 are about 3 % lower for the lower step when they were measured on the models spanning only 75 % of the tunnel width. The peak pressure ratios obtained on the models with free ends are slightly (3-5 %) below those obtained on the models which were sealed against the tunnel walls.

The static to total pressure ratio before interaction has also been recorded over the range of stagnation pressures employed (Fig.6). A mean value of $p_1/p_{01} \approx 0.011$ has been found and the corresponding initial Mach number $M_1=3.62$ has been attributed to the peak pressure ratios in Fig.5.

The influence of flow inclination on the peak pressure ratio also was checked by varying the angle of incidence of the model between -2 and +2 degrees, Fig.
The peak pressure dependence on the angle of attack can be estimated to be

$$\frac{\partial\left(\frac{p_p-p_1}{p_1}\right)}{\partial\alpha} = \frac{\partial\left(\frac{p_p-p_1}{p_1}\right)}{\partial M_1} \quad \frac{\partial M_1}{\partial\alpha} \qquad (6)$$

When $\partial\left(\frac{p_p-p_1}{p_1}\right)/\partial M_1$ is taken from Eq.(3) for a separation angle of $\theta_s=13°$ and $\partial M_1/\partial\alpha$ from isentropic flow tables at $M_1=3.62$ then

$$\frac{\partial\left(\frac{p_p-p_1}{p_1}\right)}{\partial\alpha} = .052 \text{ deg}^{-1}$$

The measurements (Fig.7) confirm the value showing that only the variation in Mach number influences the peak pressure ratio.

4.2. Cone-Cylinder-Step Models

The wall pressure distributions on the axisymmetric models at tunnel stagnation pressures between 8 and 17 kg/cm^2 and for two step heights 5 and 7.5 mm are shown in Figs.9a-b, the step face coordinate being enlarged four times. The variation of the peak pressure with tunnel stagnation pressure is

plotted in Fig.4 and the peak pressure ratio obtained at the highest tested stagnation pressures are also shown in Fig.5.

Here a stronger variation of the peak pressure with p_{0_∞} was observed. At the highest tested p_{0_∞} the measured peak pressure ratio is within a few percent the same as the one obtained on the two-dimensional models at VKI and by other investigators. At the lowest tested p_{0_∞} they are however by about 30 % higher. The variation seems to indicate a still transitional behaviour of the boundary layer.

There was no influence of the step height observed. The initial pressure ratio p_1/p_{01} also was recorded. It rises from about .009 at p_1=8 kg/cm^2 to .010 at 15 kg/cm^2 (Fig.6). In the composite diagramme (Fig.5) the initial Mach number M_1=3.70 has been attributed to the peak pressure ratios obtained at the highest p_{0_∞}.

The Reynolds number at the interaction point was not evaluated in this case since the boundary layer was undergoing the change from conical to axisymmetric flow in the expansion fan at the shoulder of the model. The boundary layer development length down to the point of interaction was longer than the one on the planar models. The peak pressure ratio observed at the highest p_{0_∞} again corresponds well to the two-dimensional results and to the values given by Eqs.(2) and (3).

The influence of the angle of attack has also been checked on this configuration. The results are presented in Fig.8. The peak pressure shows a much stronger dependence on the angle of attack due to the three-dimensionality of the flow than Eq.(6) would predict.

4.3. Axisymmetric Internal Flow Models

The wall pressure distribution on those models was measured at various positions of the step with respect to the nozzle exit plane (Figs.10,11,12) and in two cases the position was kept constant (x/D=2.0) and the stagnation pressure was varied (Figs.13,14). The initial Mach numbers were determined by the static to total pressure ratios when the 75 mm nozzle was used. It was found to be 4.83 for the step location at x/D=2.0. In the ejector set-up the jet boundary Mach number was first determined by the base pressure to total pressure ratio and then the shroud wall Mach number was determined by the two-dimensional oblique shock relation for the measured pressure rise. The initial Mach numbers M_1 were thus determined to be 4.0 (45 mm nozzle) and 4.15 (60 mm nozzle).

The diffuser wall pressure behind the 75 mm nozzle showed a small pressure drop. A gradient of $\partial(p/p_0)/\partial(x/D) \approx .65 \cdot 10^{-3}$ can be estimated from the pressure readings. The other nozzles produced a remarkably constant diffuser wall pressure confirming that the flow in the nozzle exit is uniform.

Practically no dependence of the peak pressure on unit Reynolds number was observed (Figs.13,14). The axial location of the step also had only a small and random influence on the pressure distribution in the separated flow region.

The peak pressure ratio as a function of initial Mach number compares well with other data taken in the same Mach number range and with Eqs.(2,3) (Fig.5).

4.4. Flow Visualizations

The flow around the models in tunnel S4 was examined by the schlieren and the shadowgraph techniques (Fig.18). At tunnel stagnation pressures of 12 and 13 kg/cm^2, the photographs show a similar flow pattern for all geometries :

- A slightly wavy shock wave at separation indicating unsteady flow - a roughly straight line between the approximate location of separation and a point slightly above the outer corner of the step which indicates the upper mixing region.
- A second shock wave near the reattachment at the outer corner which intereferes with the expansion fan issuing from the corner.

The ratio step height to boundary layer thickness h/δ can be estimated from those photographs to be 3 to 4.

An oil flow technique has been used to visualise the surface flow pattern on the models in tunnel S4 and in the ejector facility. On the planar models which were sealed against the tunnel wall, the following oil motion was observed during the tests :

- An irregular but symmetric separation line was formed as shown in Fig.19.
- Two rather important vortices were situated close together on the tunnel wall and on the model surface.
- Several other vortices were located behind the separation line as indicated in Fig.19.
- A very straight separation line was observed at about 20 % of the step height indicating a small vortex which is located in the corner. At this oil accumulation line small irregularly distributed vortices were also observed.

The two-dimensional model with free ends : The oil accumulation line at separation on this model showed smaller disturbances than the one described before. Similar but smaller vortices were observed behind the separation line. In total the separation line looked more "two-dimensional" having less disturbances and approaching more a straight line.

Cone-cylinder step models : Here the separation line was rather straight over about 70% of the circumference. Two rather large vortices were observed on either side of the model and were spaced at 180° (Figs.20a-b). A regular separation line on the step face (y/h = 20 %) with small vortices on it has also been observed. During the visualization test the angle of incidence of the model was altered. The oil pattern and the oil motion was only little influenced hereby. The same oil flow pattern was obtained when the axial location of the model in the test section was changed.

Axisymmetric internal flow models : Here essentially the same phenomena have been observed. A regular separation line on about 20 % of the step height. A rather regular separation line (compared to the above-mentioned models) and smaller vortices behind that separation line. The separation θ_s angle here was smaller (10...11 degrees) when determined from oil accumulation at separation and the step height.

4.5. The Pressure Distribution and the Pressure Integral Over the Step Face

One of the major objectives of the experiments presented here was to find a general rule for the step pressure integral as a function of the main parameters - relative step height and Mach number. The measured pressure distribution in the ejector facility is plotted versus the cross sectioned area which is normalized by the throat area (Fig.15).

All cases show a similar behaviour at different pressure levels. The integration has been carried out graphically and the resulting values are shown in Fig.17 under the dimensionless form

$$\frac{D}{p_1 \Delta A} = \int_{\text{step}} \frac{p}{p_1} \frac{dA}{\Delta A} \qquad (7)$$

The pressure distribution obtained from the two-dimensional and axisymmetric models in tunnel S-4 are presented in Fig.16. For the planar models a mean value can be defined around which the measured data scatter by about $\pm$ 5%. The pressure variation is in general the same as observed by Bogdonoff (Ref.1) and Sterret (Ref.4).

The integration

$$\int \frac{p}{p_1} \frac{dy}{h} = \frac{D}{p_1 h} \qquad (8)$$

has been carried out graphically and the result is also indicated in Fig.17.

In the same figure finally the step pressure integrals from measurements by Bogdonoff (Ref.1) and Sterret (Ref.4) are included. Heyser et al. (Ref.14) measured the force acting on the step with a strain gauge balance. All the data indicate a linear variation of the step pressure integral in the Mach number range between 2 and 6 having the approximate form

$$\int \frac{p}{p_1} \frac{dy}{h} \approx 1.1\, M_1$$

Step pressure data obtained from another test programme carried out independently at VKI at $M_1 = 2$ on planar models which completely spanned the wind

tunnel with a boundary layer trip near the leading edge are included in Figs. 5, 16 and 17. The step pressure distribution has the expected level and the step pressure integral agrees with Eq.(9).

4.6. Discussion

The variation of the peak pressure ratio, induced side force and induced drag clearly shows a linear variation with Mach number. A 10 % scatter of the experimental results about the mean values has been found to be typical. Test results obtained at VKI were repeatable. An eventual influence of the unsteadiness of the flow, therefore, can be eliminated as a possible reason for the scatter of the results.

Other parameters must be considered to explain the scatter of all the experimental data; e.g., three-dimensional effects in two-dimensional and axisymmetric flows. A real two-dimensional situation has not been achieved in all the experiments conducted so far. Side fences as well as free ends on two-dimensional models have displayed three-dimensional effects. Also axisymmetric internal and external flow models have irregularly distributed vortices behind the also irregular separation line. Those flow irregularities which seem to be independent of the model geometry and strongly connected to the separation process itself already could be the reason for a non-uniform lateral pressure distribution and lateral flows. They would explain a certain scatter of the measured pressures. Experiments on highly three-dimensional models have shown that lateral flows affect the pressure distribution on the axis of symmetry only to a certain degree but never dominate the Mach number dependence of the pressure distribution.

Other sources of errors in correlating peak pressure and induced forces with Mach number are the uncertainties in the tunnel Mach number and the relative flow inclination. The tunnel free stream Mach number changes over larger stagnation pressure ranges due to the change in nozzle boundary layer displacement thickness and the resulting effective nozzle contour. In two-dimensional flows the effect of flow inclination can be related to a corresponding Mach number variation. On axisymmetric models the cross flow caused a bigger effect of the angle of attack in the pressure variation.

Reynolds number effects on the characteristic pressure were found to be present at higher values of Reynolds number than previously reported. However, different conditions in wind tunnels and on the tested models can produce the slight Reynolds number influence which was found in some parts of the present research. Tripped boundary layers, finally, are known to introduce additional effects into the flow and cannot be compared directly to boundary layer which have undergone a "natural" transition.

Previous investigations as well as the present one have shown that the relative step height has no influence on the characteristics pressures in the separated flow region if h/δ is larger than one and below a certain limit which depends on Mach number. Three regimes of relative step height can be roughly separated so far. When the step height is smaller than the boundary layer thickness the pressure level of the characteristic pressures depends strongly on the step height as Bogdonoff (Ref.1) has shown. A similarity in the pressure distribution exists in the second regime when h/δ lies between one and the upper limit. Here the pressure level is linearly related to the Mach number. For larger step heights the pressure on the outer portion of the step, particularly at hypersonic

Mach numbers, is strongly influenced by the step height and the Mach number (Refs.4-5).

The linear variation of characteristic pressures and forces with Mach number for the second step height regime and for Mach numbers between 2 and 6 has been confirmed by many investigators. A suitable physical model describing the experimental results is still locking. The oblique shock relations which could be used to determine the pressure level in the separated flow region imply the separation angle as a parameter. The separation angle has been found to be approximately 13° and roughly constant. There are, however, indications that the separation angle decreases with higher Mach numbers (oil flow pictures in the internal flow facility indicated $\theta_s=11°$ at M=4.8). A decreasing separation angle would explain the linear variation of the pressure with Mach number together with the quadratic oblique shock relations.

Difficulties in determining experimentally the separation point and the correct inclination of the shear layer are still the main problem to a correct answer to this type of separated flow.

5. CONCLUSIONS

The results of the present experimental program in conjunction with the work of previous investigators lead to the following conclusions :

i there is no essential difference in the pressure distribution in the separated flow region ahead of steps in axisymmetric internal and external flow and on two-dimensional and three-dimensional configurations.

ii A similarity exists in the pressure distribution throughout the whole separated flow region for turbulent flow and within a certain limit of the relative step heights.

iii Above a certain Reynolds number and for step height ratios $h/\delta > 1$ at Mach numbers between 2 and 6, the peak pressure ratio p_p/p_1, the induced side force and the step pressure integral were found empirically to be linear functions of the Mach number.

iv A step-type contraction in supersonic diffusers of ejectors (second throat) can be used in order to improve pressure recovery. The law for the step pressure integral allows one to predict the pressure recovery.

REFERENCES

1. BOGDONOFF, S.M., and KEPLER, C.E., Interaction of a turbulent boundary layer with a step at M=3, Princeton Univ. Report 238, 1953.

2. CHAPMAN, D.R., KUEHN, D.M., LARSON, H.K., Investigation of separated flows in supersonic and subsonic streams with emphasis on the effect of transition, NACA TN 3869, 1957.

3. MAURER, F., Three-dimensional effects in shock separated flow regions ahead of lateral control jets issuing from slot nozzles of finite length. Separated Flows Part 2, Proc. of a Specialists' Meeting, AGARD Fluid Dynamics Panel (AGARD, Paris, France, 1966).

4. STERRET, J.R., and BARBER, J.B., A theoretical and experimental investigation of secondary jets in a Mach 6 free stream with emphasis on the structure of the jet and separation ahead of the jet, Separated Flows Part 2, Proc. of a Specialists' Meeting, AGARD Fluid Dynamics Panel (AGARD, Paris, France, 1966).

5. WESTKAEMPER, J.C., Turbulant boundary layer separation ahead of cylinders, AIAA J. 6, 1968.

6. BERNSTEINE, H., and BRUNK, W.E., Explorating investigation of the flow in the separated region ahead of two blunt bodies at Mach number 2, NACA RM E55 D076, June 1955.

7. JOHNSTON, S.C., Experimental investigation of a supersonic air-air ejector operating with a second throat. VKI TN 45, von Karman Institute, Rhode-Saint-Genèse, Belgium.

8. LOVE, E.S., Pressure rise associated with shock induced boundary layer separation, NACA TN 3601, 1955.

9. LAUGE, R.H., Present status of information relative to the prediction of shock-induced boundary layer separation, NACA TN 3055, 1954.

10. STERRETT, J.K., and EMERY, J.C., Extension of boundary layer separation criteria to a Mach number of 6.5 by utilizing flat plates with forward facing steps. NASA TN D-618, 1960.

11 BOGDONOFF, S.M., Some experimental studies of the separation of supersonic turbulent boundary layers, Princeton Univ. Report 336, 1955.

12 ABBOTT, I.H., Some factors contributing to scale effect at supersonic speeds, AGARD Memorandum AG8/M4, 1953.

13 ZUKOSKI, E.E., Turbulent boundary layer separation in front of a forward facing step, AIAA J. Vol 5, No. 10, 1967.

14 HEYSER, A. and MAURER, F., Experimentelle Untersuchungen an festen Spoilern und Strahlspoilern bei Machschen Zahlen von 0.6 bis 2.8, Zeitschrift für Flugwissenschaften, Apr/Mai, 1962.

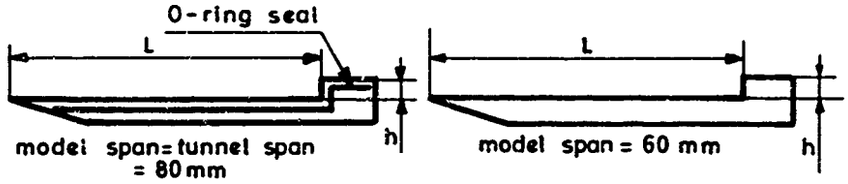

L = 120 mm h = 5 and 7,5 mm

Fig. 1 a TWO-DIMENSIONAL MODELS.

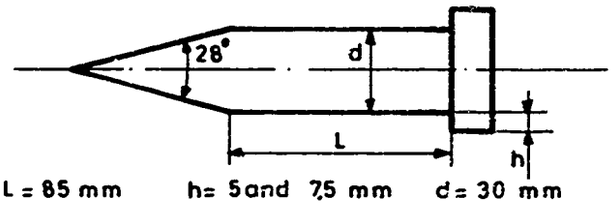

L = 85 mm h = 5 and 7,5 mm d = 30 mm

Fig. 1b AXI-SYMMETRIC MODEL.

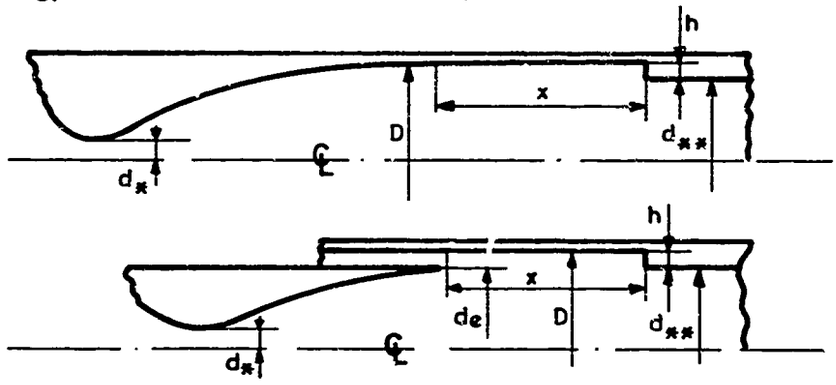

d* = 15 mm de = 45 and 60 mm D = 75 mm d** = 62 mm h = 6,5 mm
x = 0,5 . . . 2,0 D

Fig. 1c INTERNAL FLOW AND EJECTOR FACILITY.

Fig. 1 MODELS AND FACILITIES.

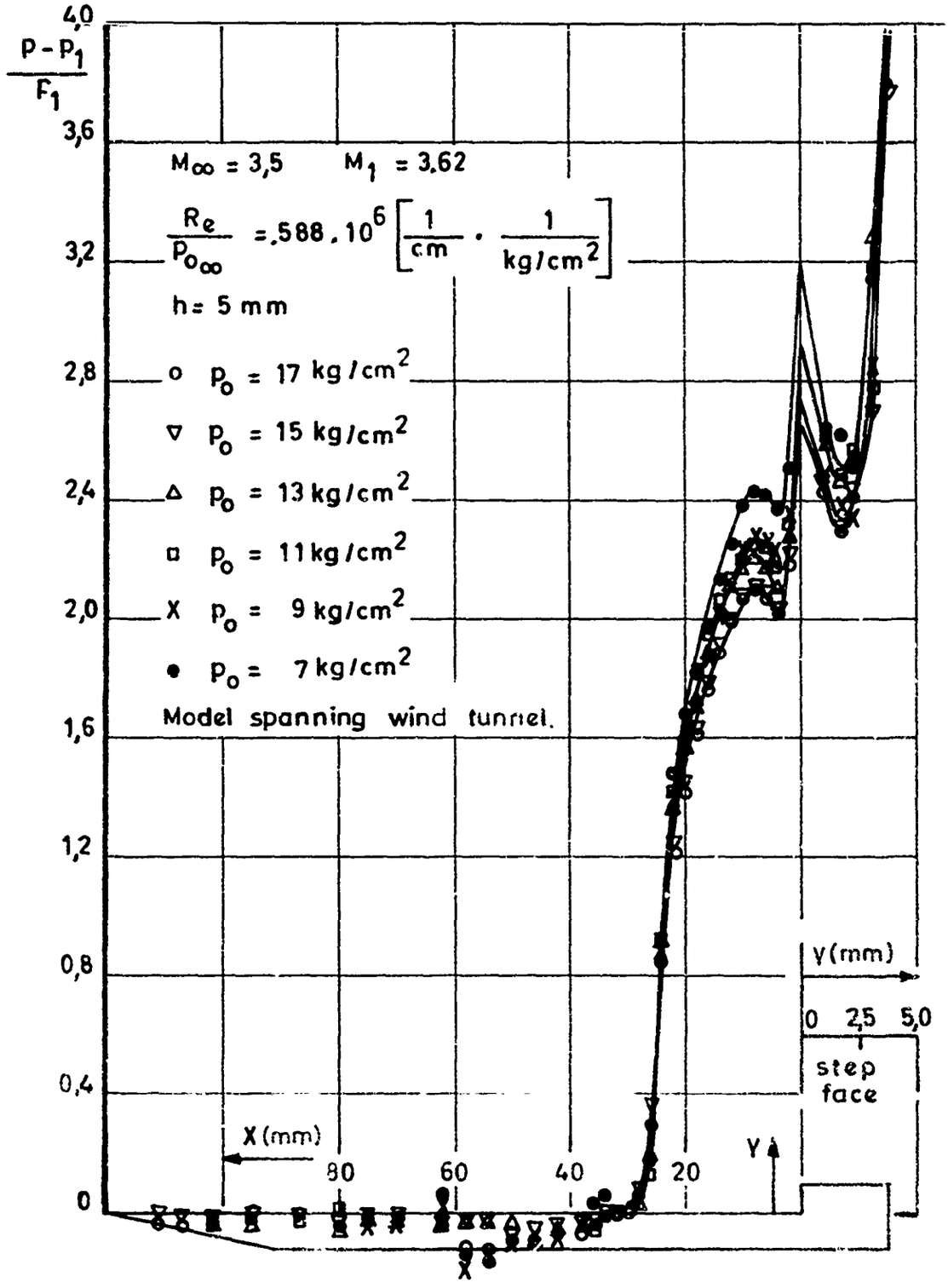

Fig. 2a WALL PRESSURE DISTRIBUTION

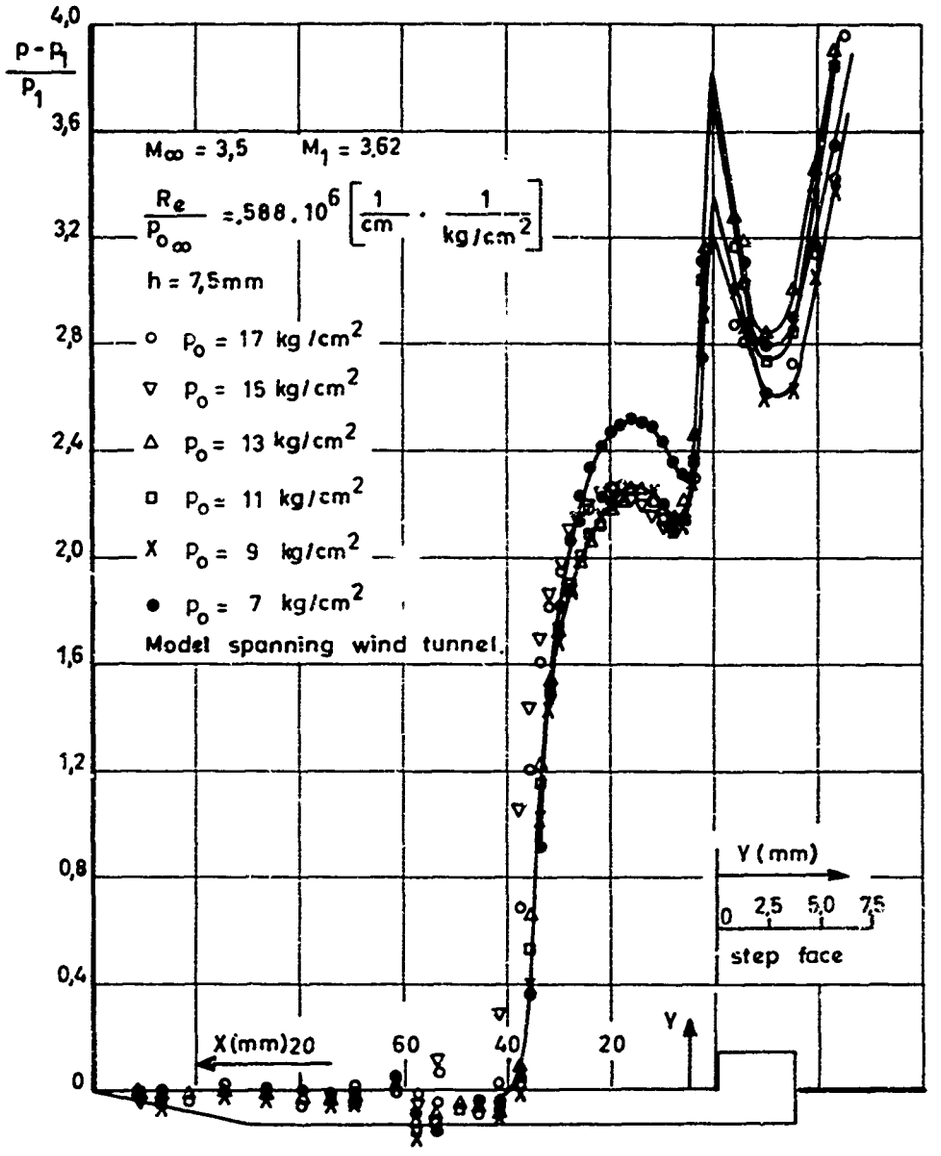

Fig. 2b WALL PRESSURE DISTRIBUTION.

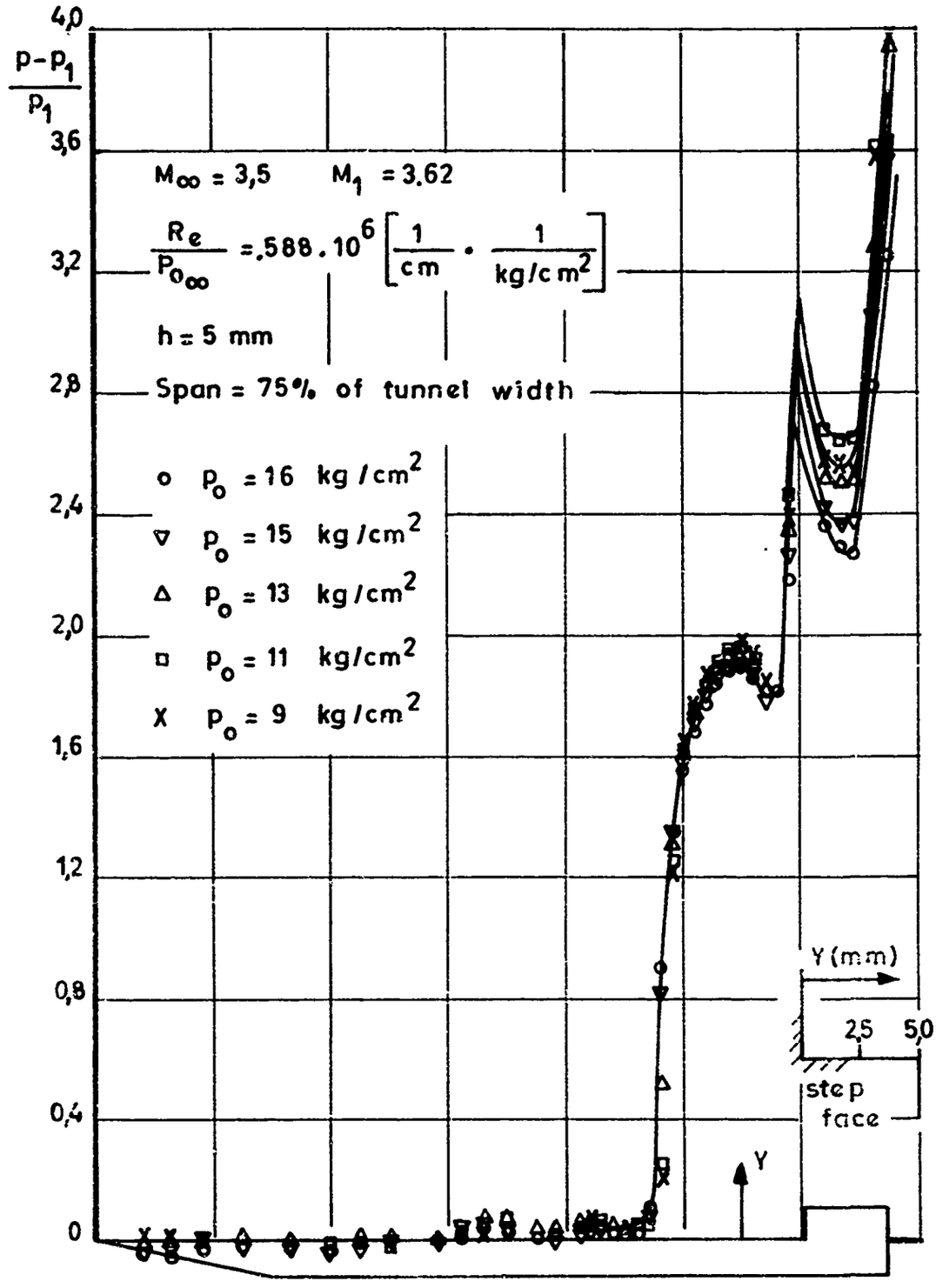

Fig. 3a WALL PRESSURE DISTRIBUTION.

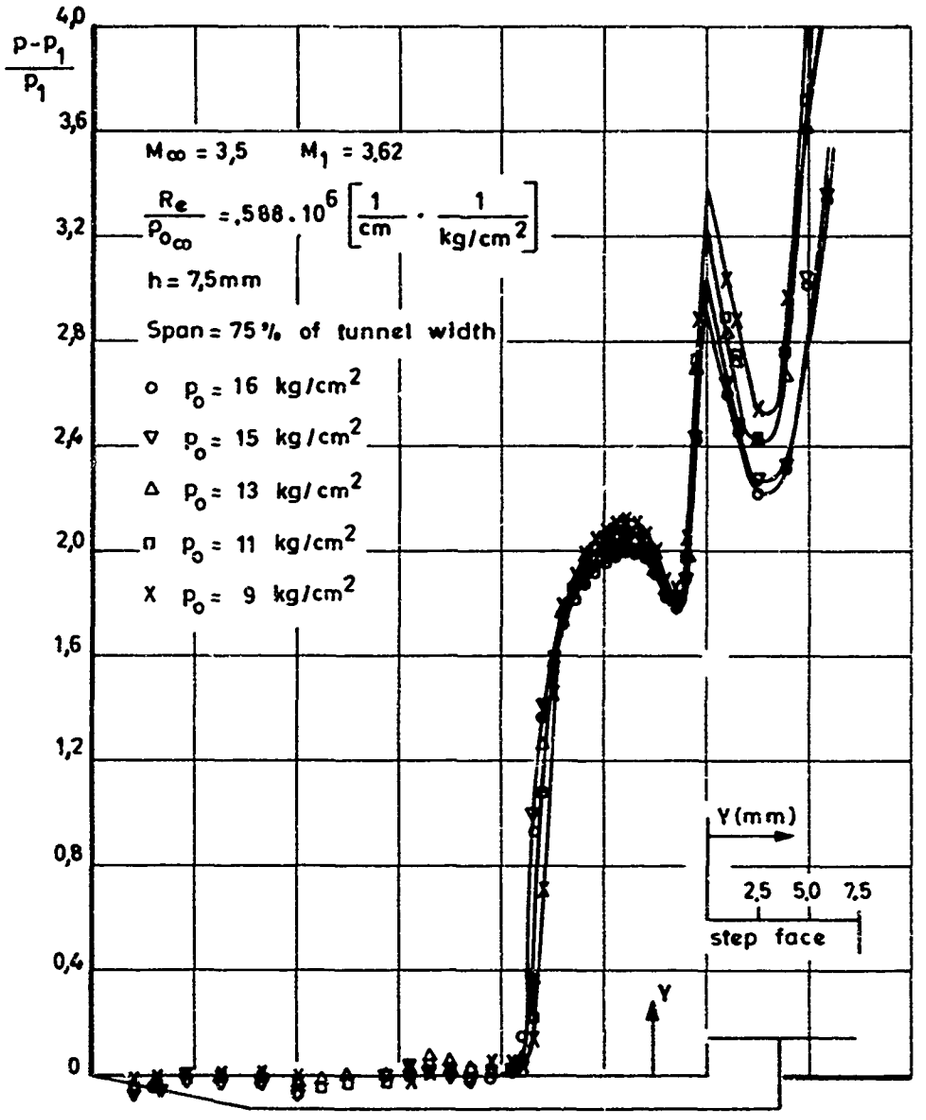

Fig. 3b WALL PRESSURE DISTRIBUTION.

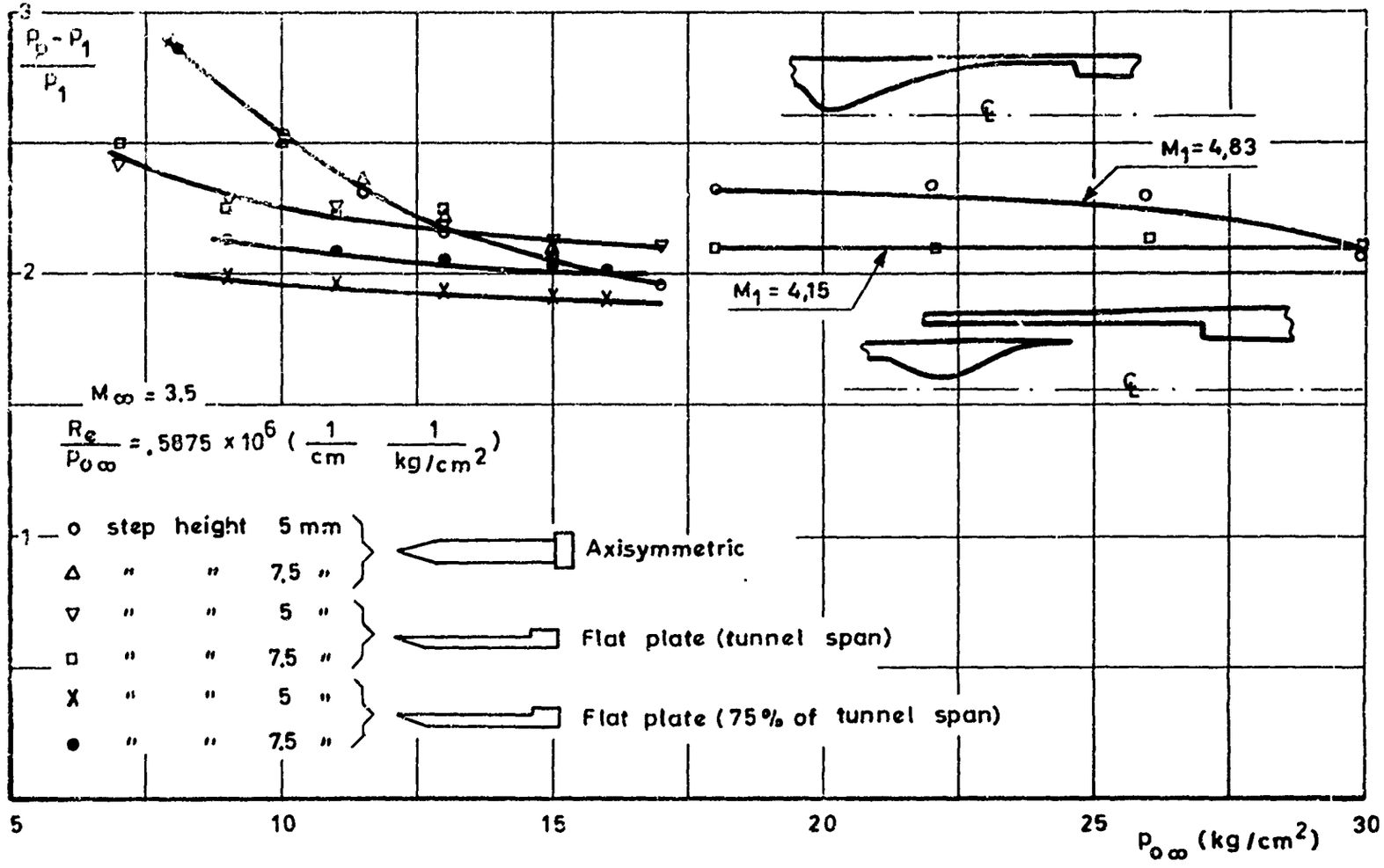

Fig. 4 VARIATION OF PEAK PRESSURE WITH REYNOLDS NUMBER

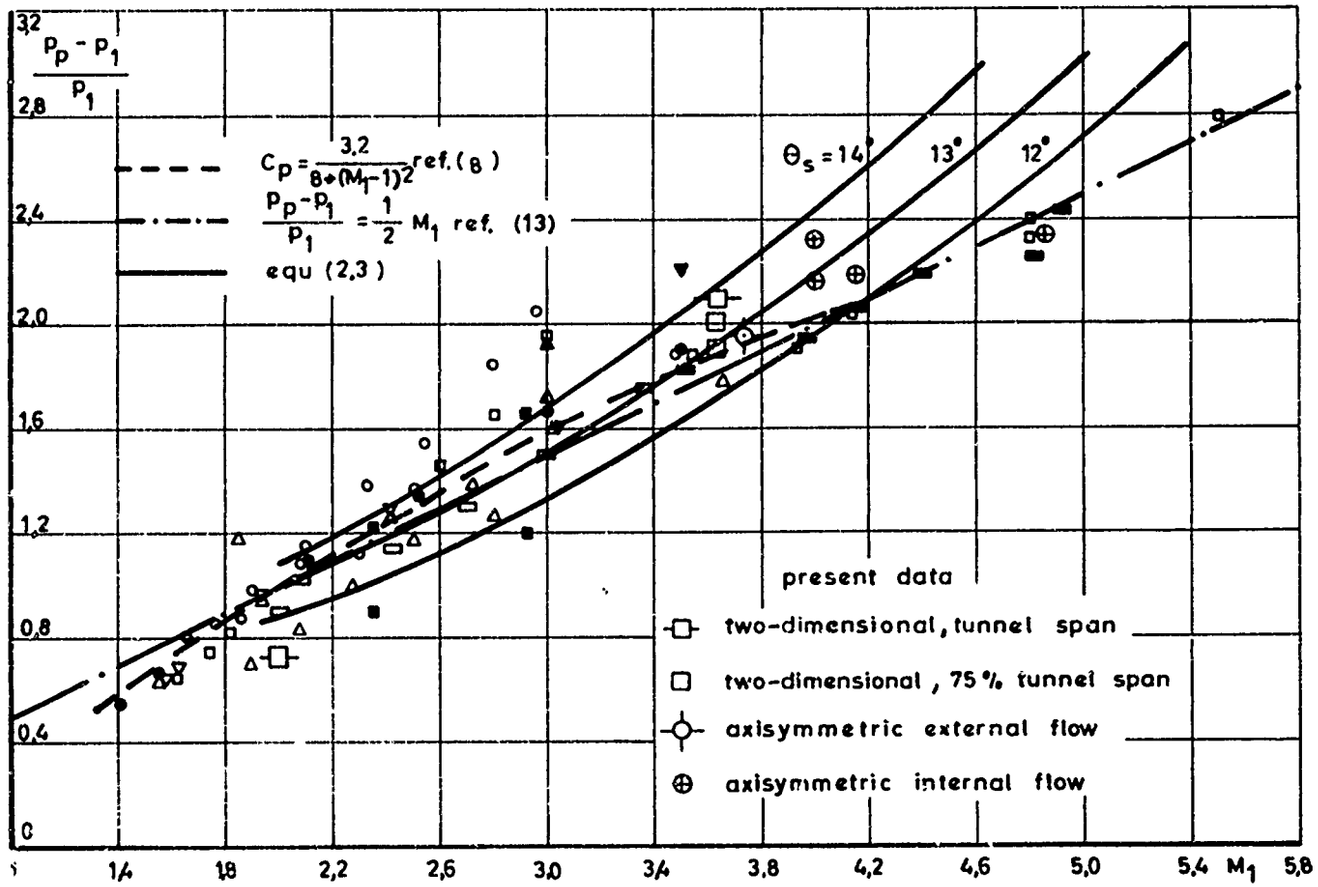

Fig. 5 VARIATION OF PEAK PRESSURE RATIO WITH MACHNUMBER. COMPOSIT OF AVAILABLE DATA.

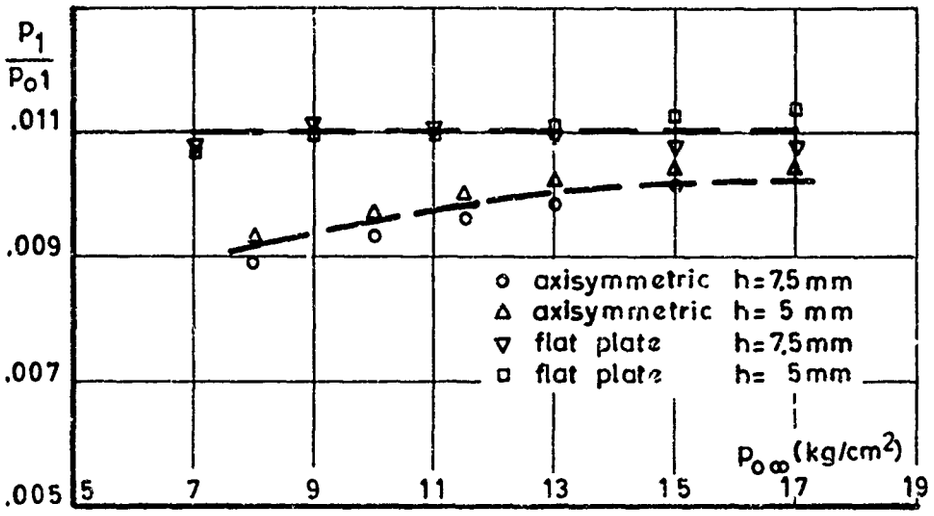

Fig. 6 INFLUENCE OF $p_{0\infty}$ ON PRESSURE RATIO BEFORE INTERACTION

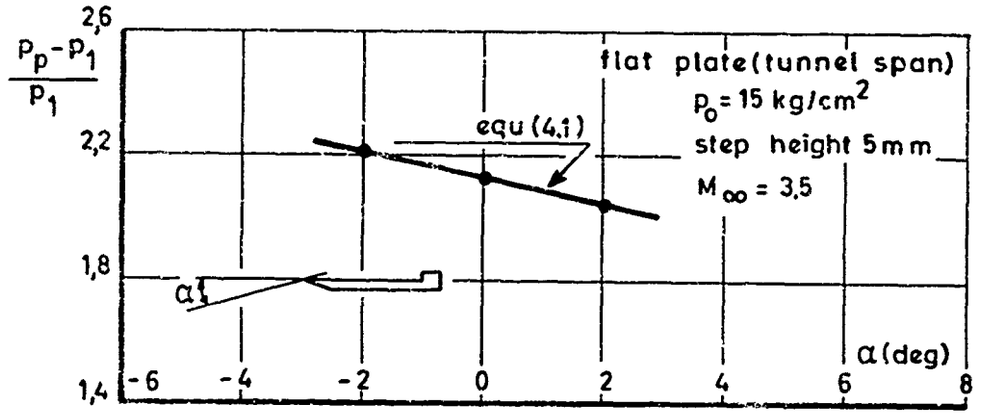

Fig. 7 INFLUENCE OF ANGLE OF ATTACK ON PEAK PRESSURE RATIO

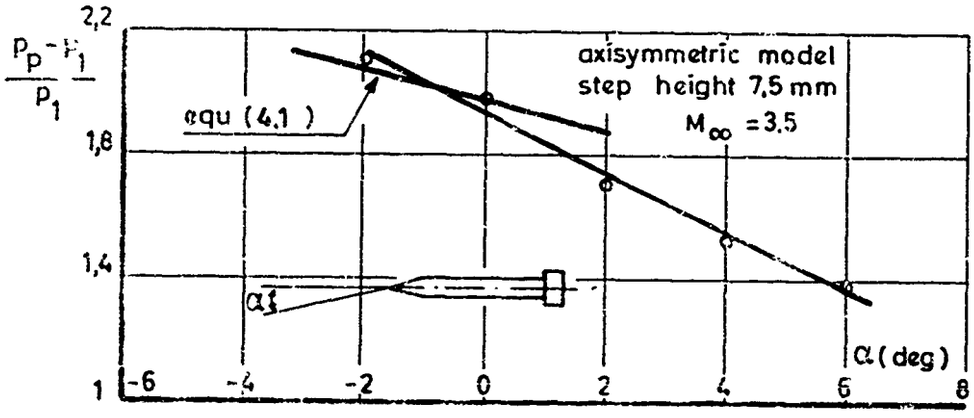

Fig. 8 INFLUENCE OF ANGLE OF ATTACK ON PEAK PRESSURE RATIO

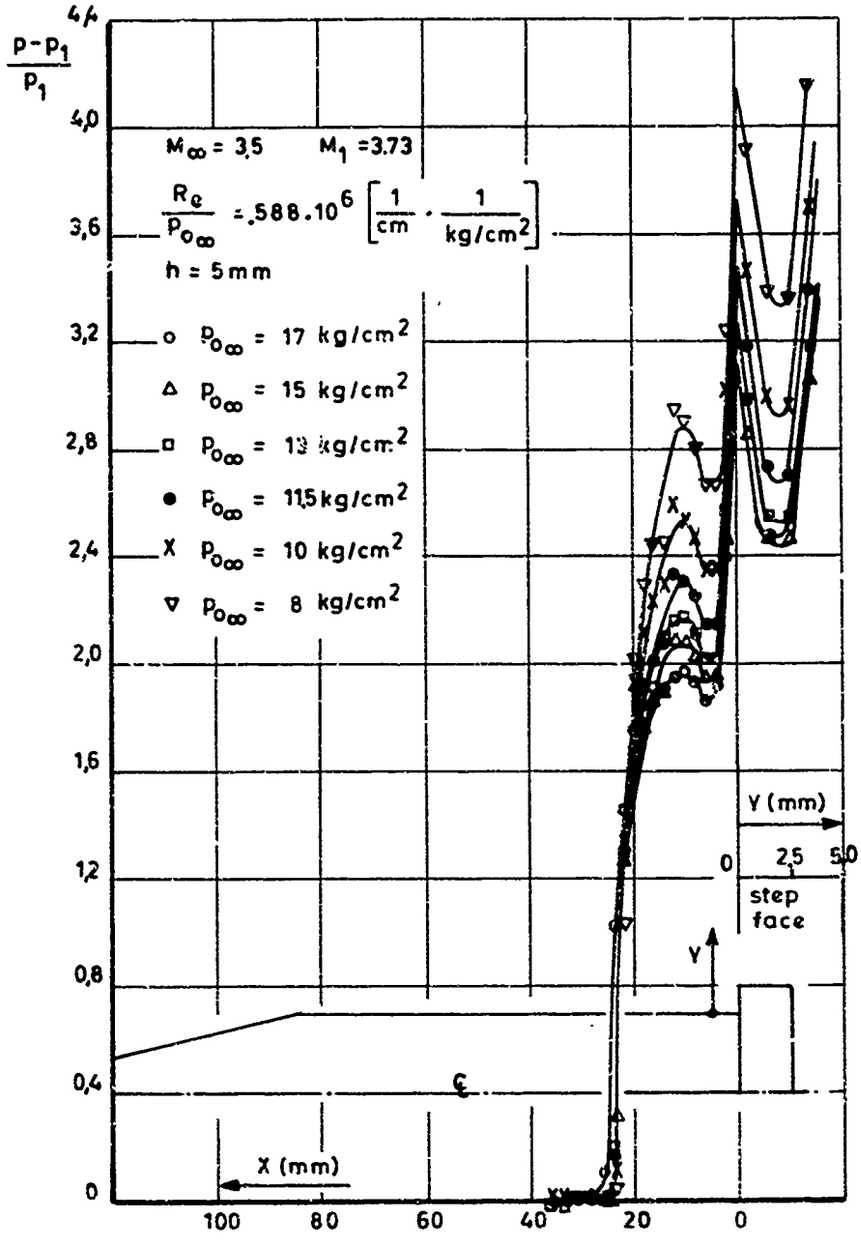

Fig. 9 a WALL PRESSURE DISTRIBUTION

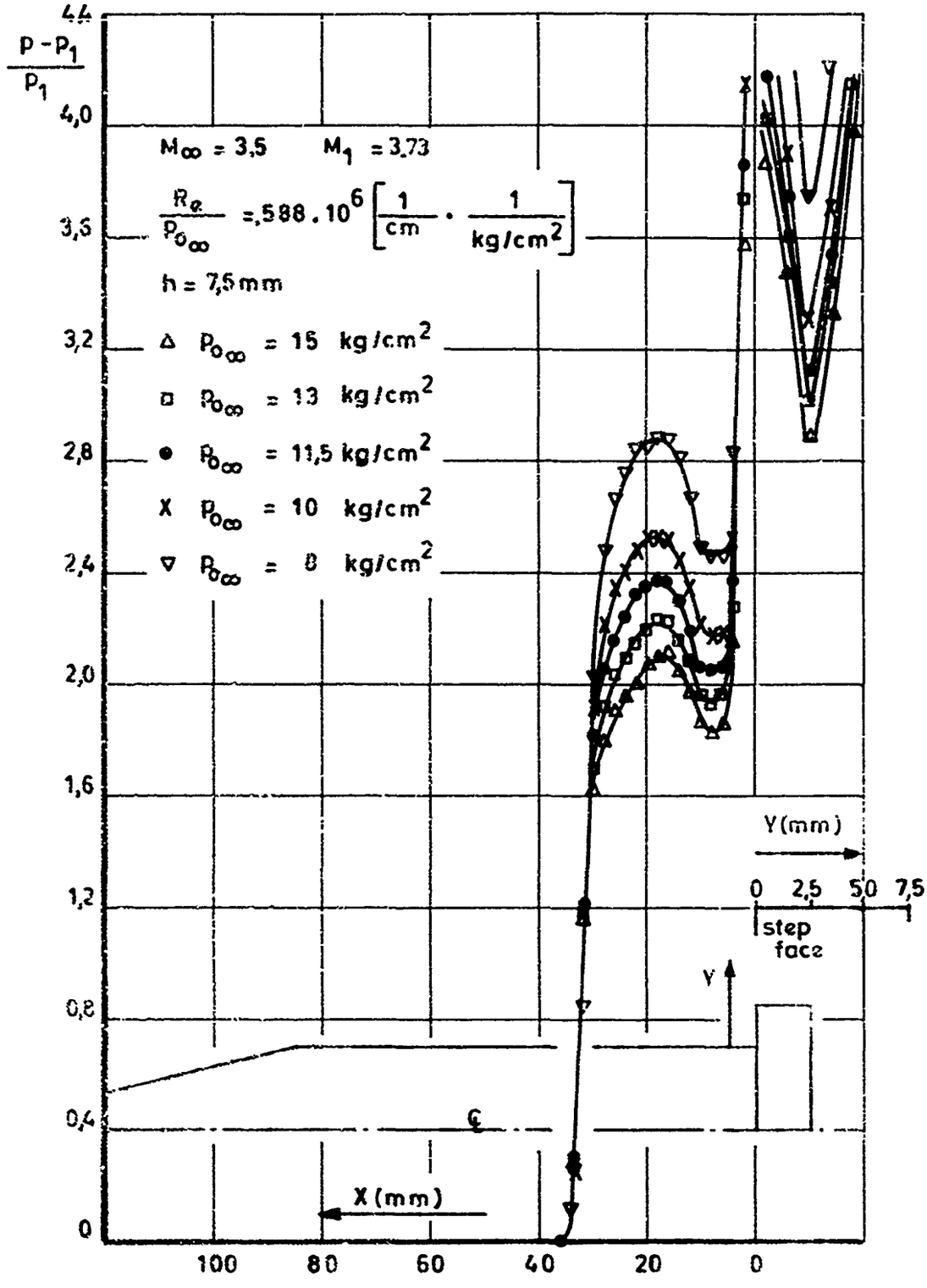

Fig. 9b WALL PRESSURE DISTRIBUTION.

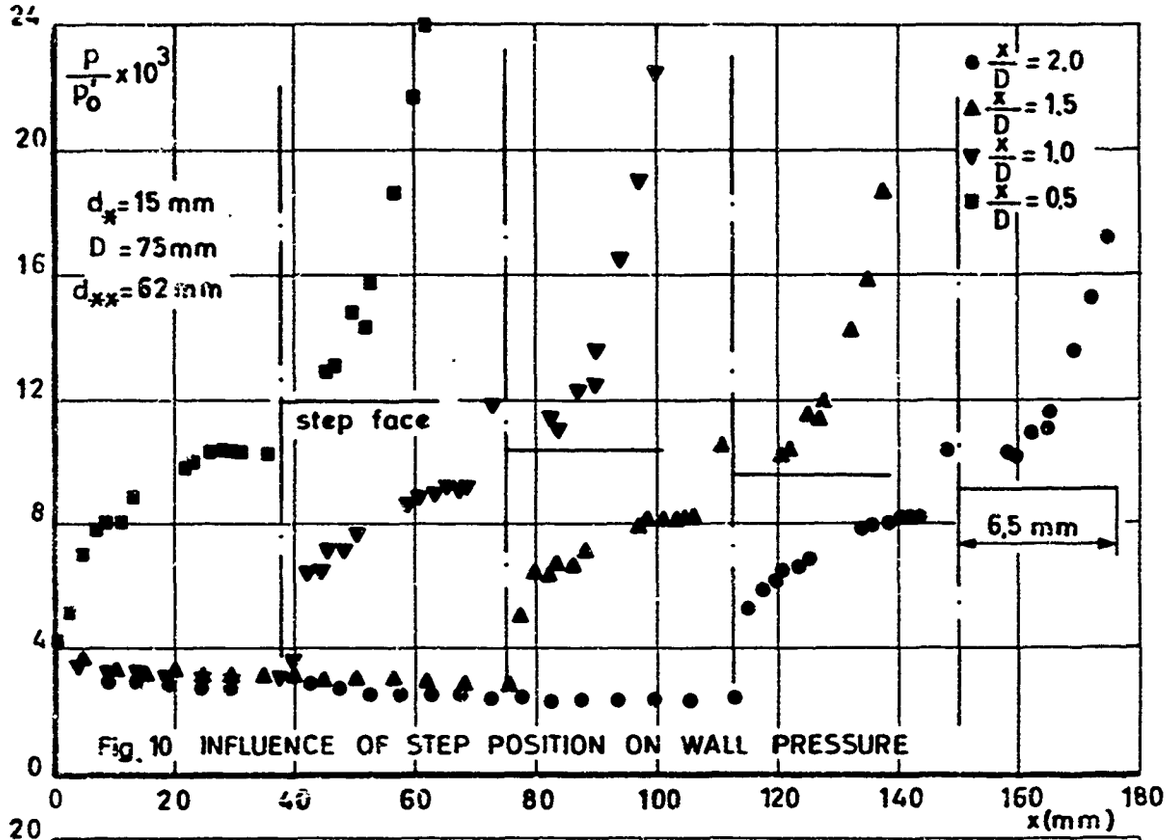

Fig. 10 INFLUENCE OF STEP POSITION ON WALL PRESSURE

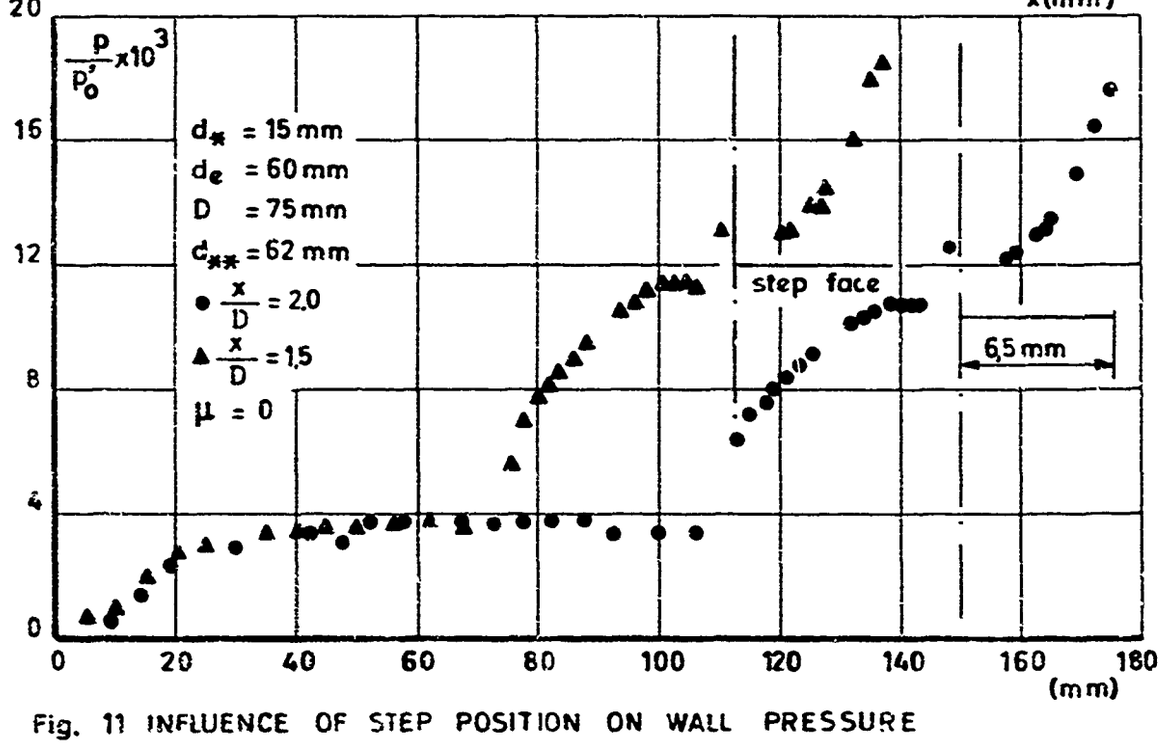

Fig. 11 INFLUENCE OF STEP POSITION ON WALL PRESSURE

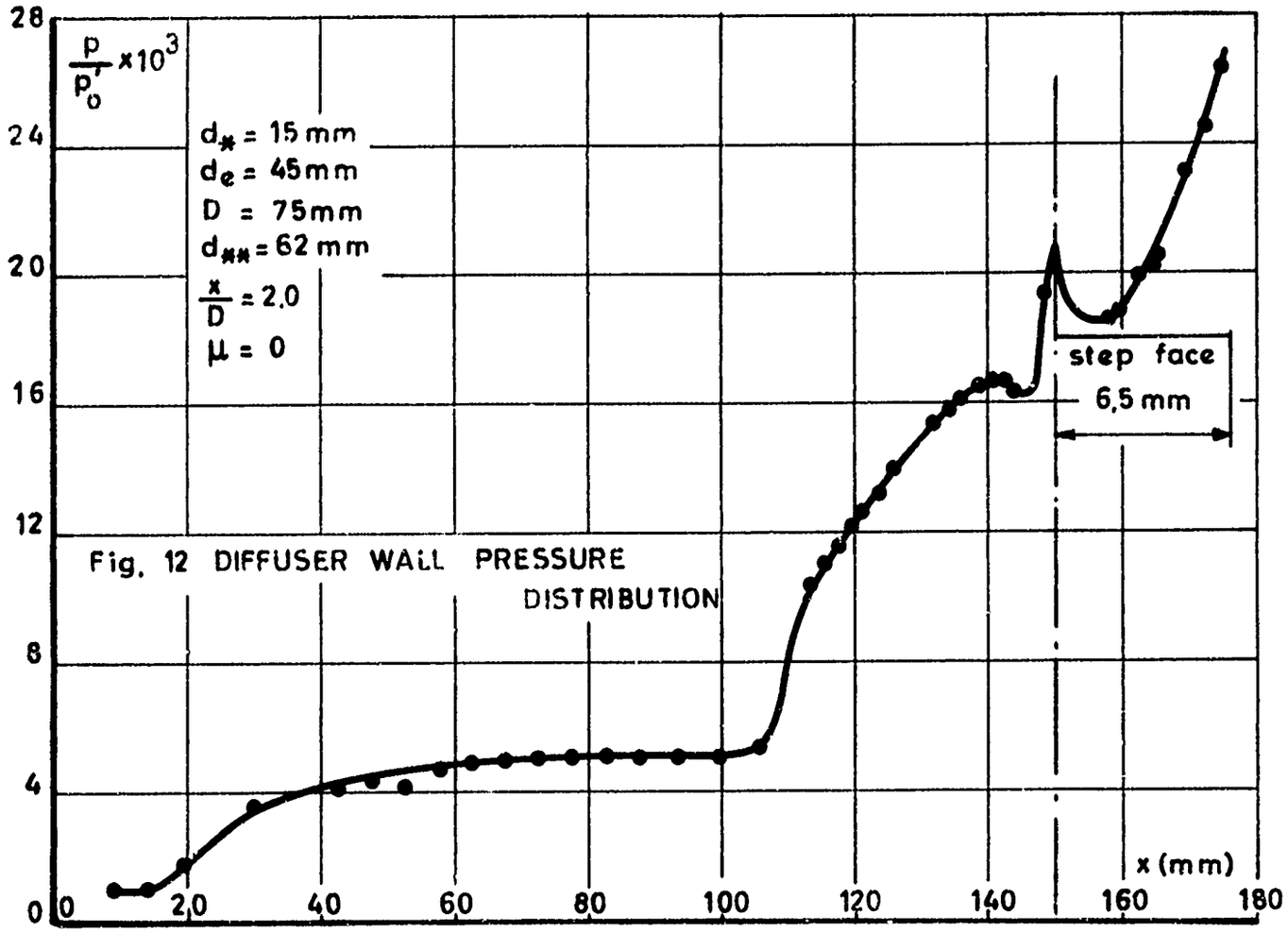

Fig. 12 DIFFUSER WALL PRESSURE DISTRIBUTION

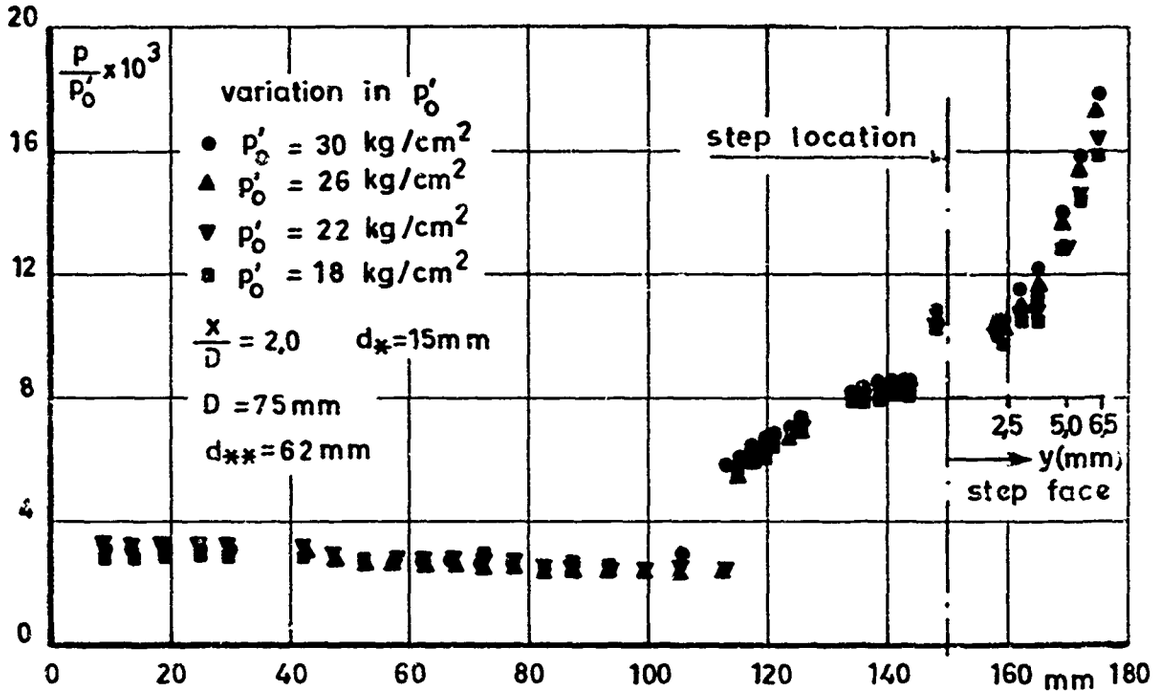

Fig. 13 WALL PRESSURE DISTRIBUTION, INFLUENCE OF STAGNATION PRESSURE.

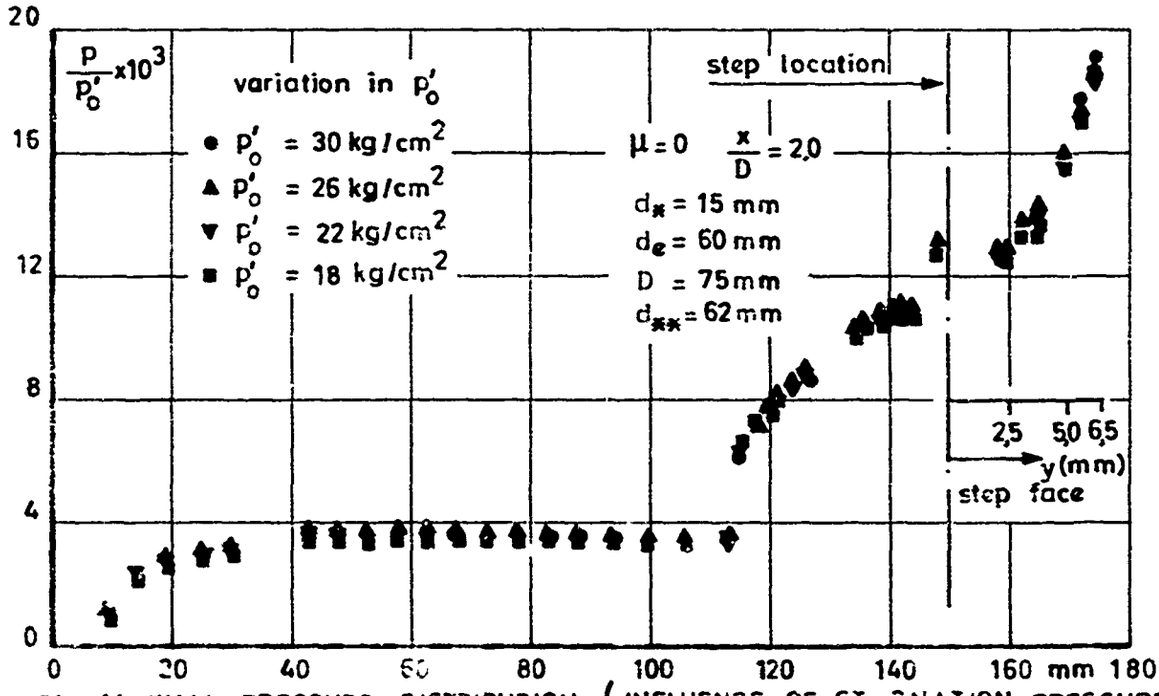

Fig. 14 WALL PRESSURE DISTRIBUTION / INFLUENCE OF STAGNATION PRESSURE

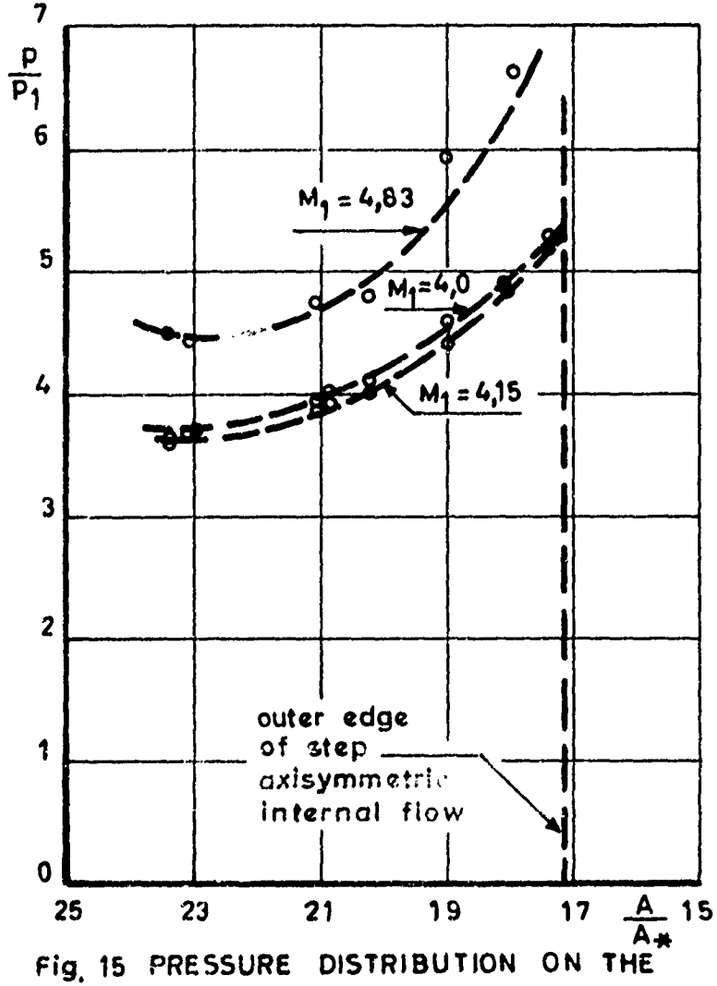

Fig. 15 PRESSURE DISTRIBUTION ON THE STEP FACE

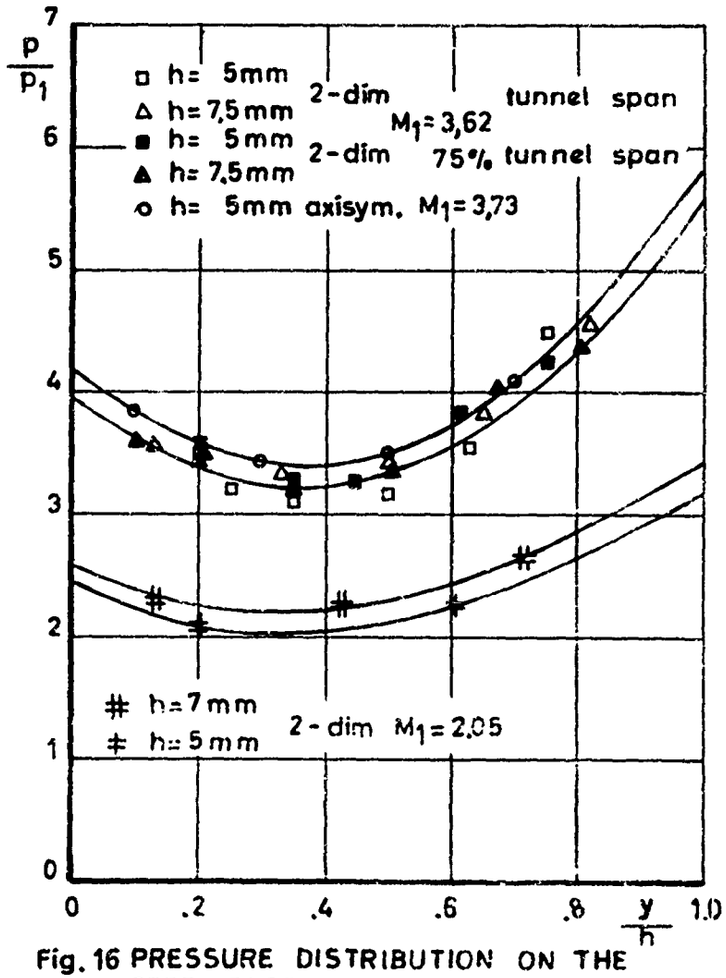

Fig. 16 PRESSURE DISTRIBUTION ON THE STEP FACE

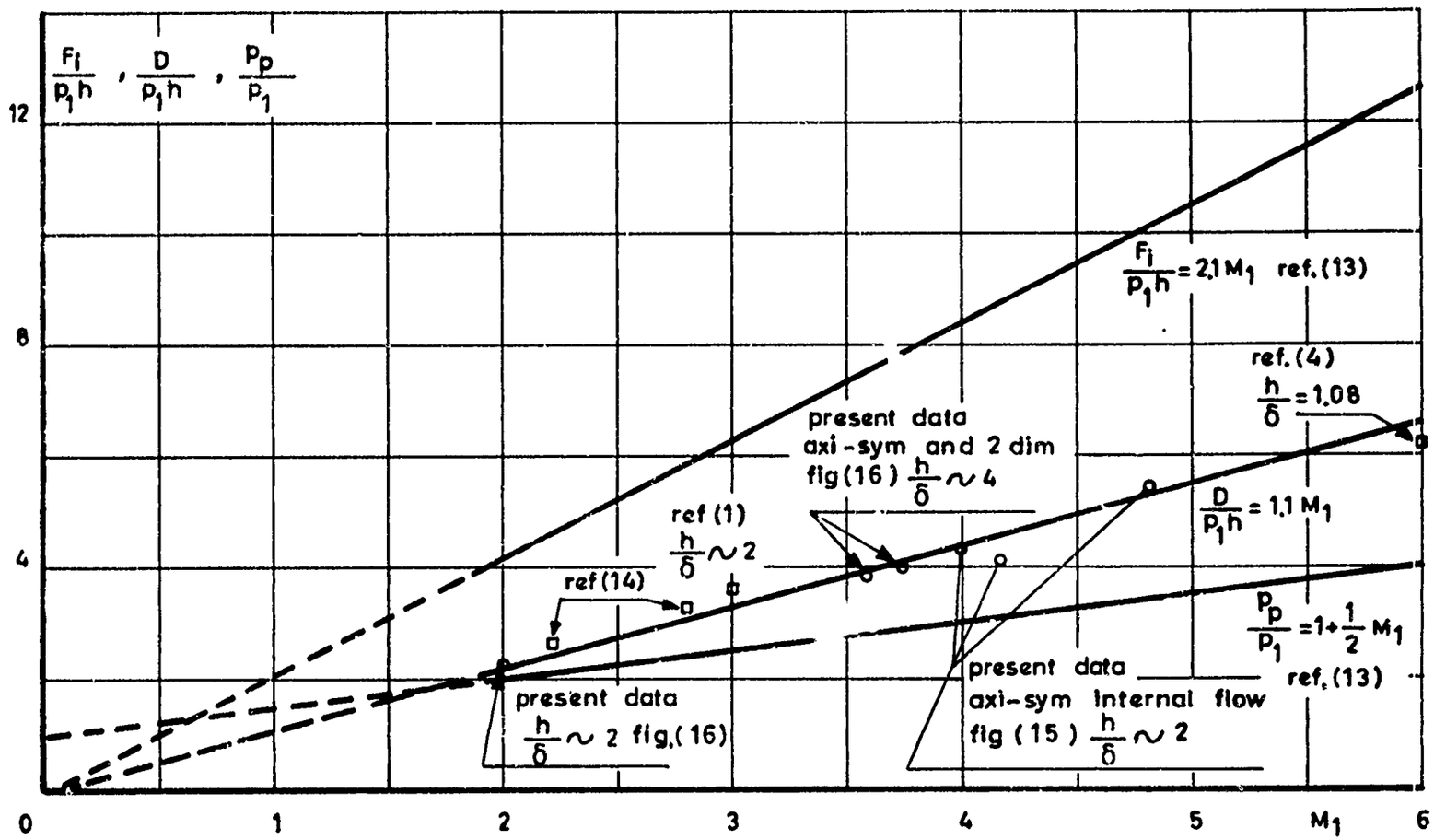

Fig. 17 PEAK PRESSURE AND INDUCED FORCES

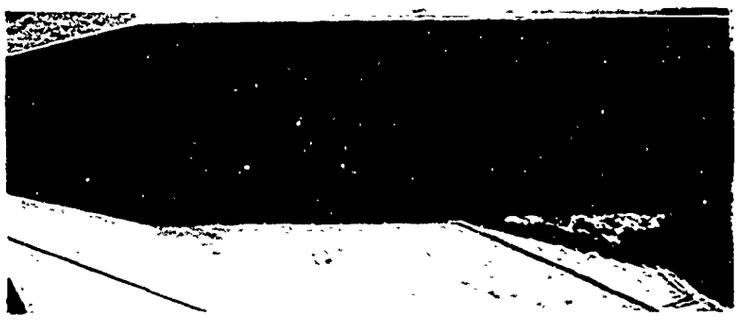

AXISYMMETRIC MODEL, SCHLIEREN PHOTOGRAPH,
$p_o = 12\,kg/cm^2$

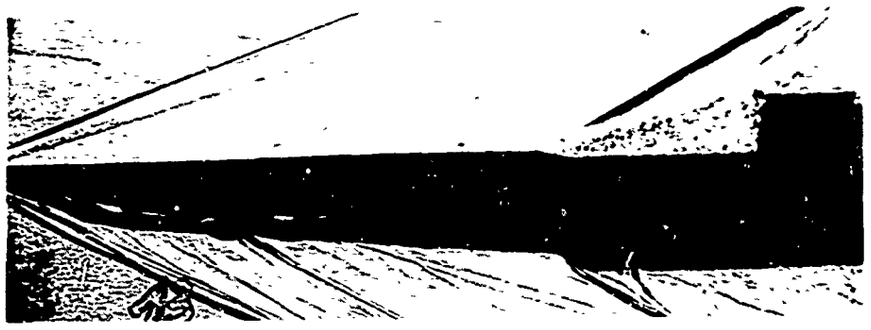

PLANAR MODEL, FREE ENDS, $p_o = 13\,kg/cm^2$, SHADOWGRAPH

PLANAR MODEL SEALED TO TUNNEL SIDE WALLS,
$p_o = 12\,kg/cm^2$ SHADOWGRAPH

Fig. 18 SCHLIEREN AND SHADOWGRAPH

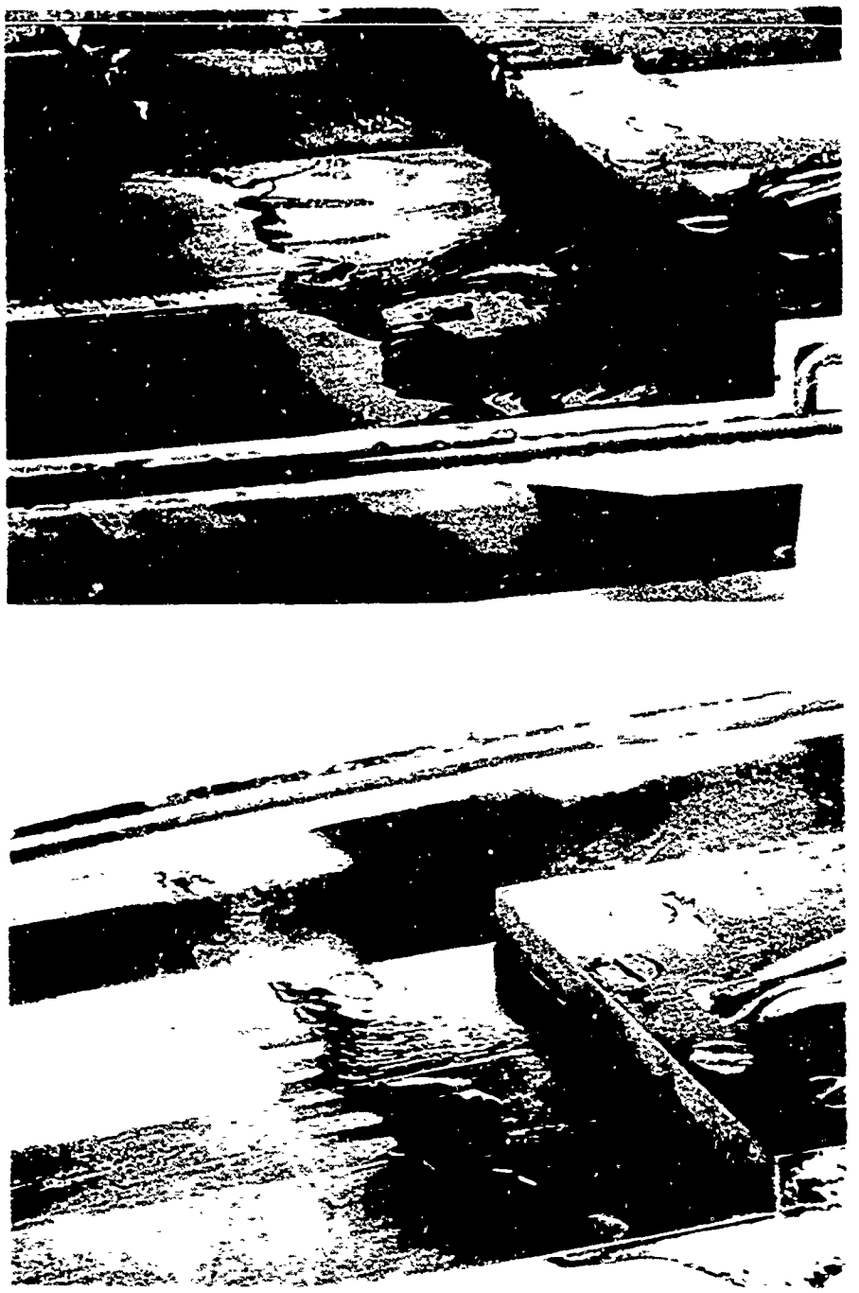

Fig. 19 SURFACE FLOW VISUALISATION BY OIL FLOW TECHNIQUE PLANAR MODELS, SEALED AGAINST TUNNEL SIDE WALLS (ABOVE) AND FREE ENDS.

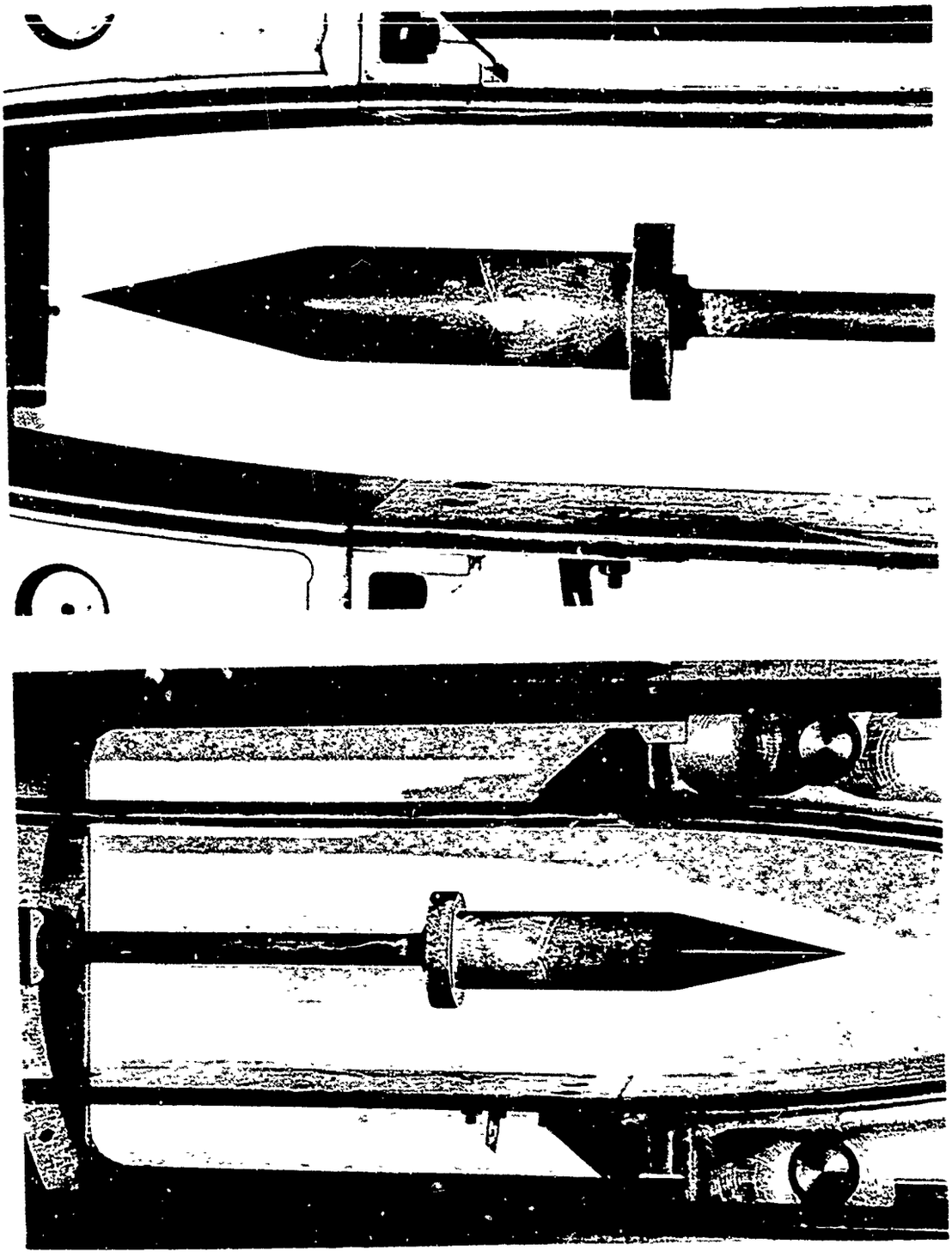

Fig. 20a SURFACE FLOW VISUALISATION BY OIL FLOW TECHNIQUE AXISYMMETRIC MODEL

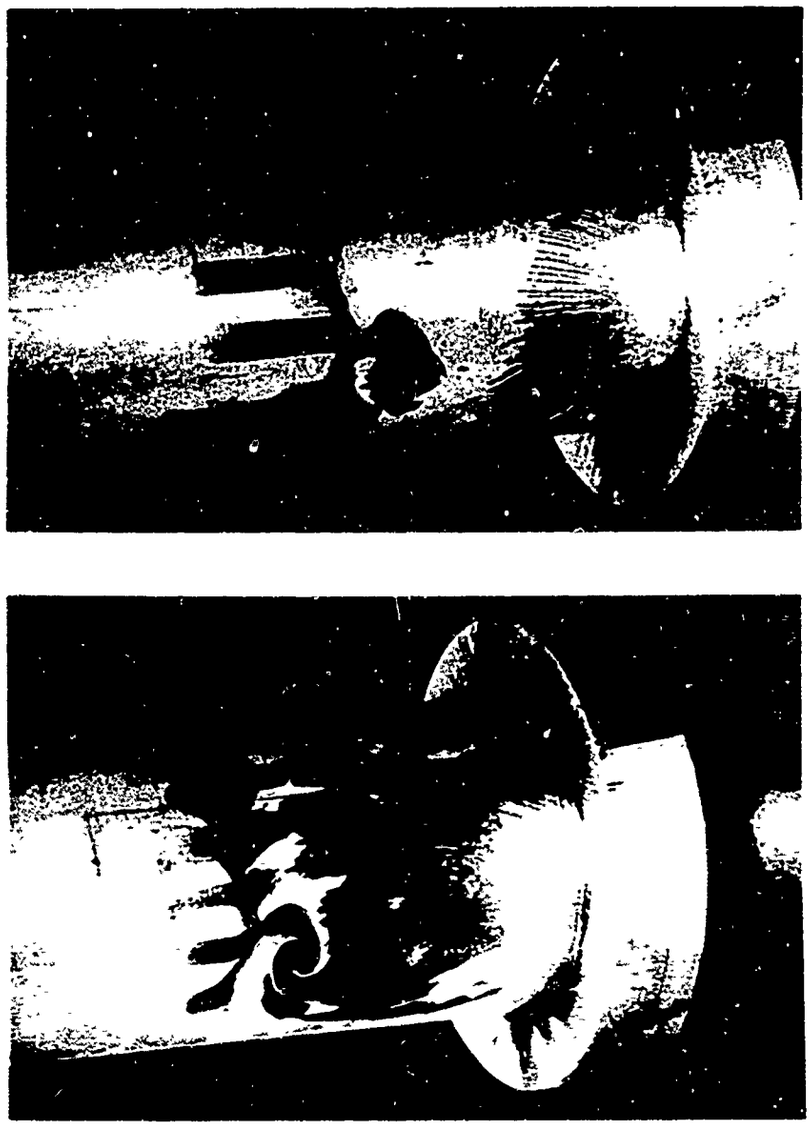

Fig. 20b SURFACE FLOW VISUALISATION BY
OIL FLOW TECHNIQUE